# Thermodynamics of nonideal cesium plasma

A. V. Bushman, B. N. Lomakin, V. A. Sechenov, V. E. Fortov, O. E. Shchekotov, and I. I. Sharipdzhanov

*All-Union Research Institute for Optical-Physical Measurements,*
*Moscow Physico-technical Institute,*
*and Institute of Chemical Physics, USSR Academy of Sciences*
(Submitted May 21, 1975)
Zh. Eksp. Teor. Fiz. **69**, 1624–1632 (November 1975)

Experiments on dynamic compression of cesium vapor are carried out with heated diaphragm shock tubes. Data pertaining to the caloric equation of state $H(P, V)$ are obtained in a broad range of the phase diagram. These data are used to calculate the shock-compression temperature and the isentropes of an nonideal plasma. The effect of strong Coulomb interaction on the thermodynamic properties of a dense plasma is studied by comparing the experimental results with theoretical models.

PACS numbers: 52.25.Kn

## 1. INTRODUCTION

Cesium is the most convenient object for the study of the influence of a strong electrostatic interaction on the thermophysical characteristics of a plasma, because its low ($I \sim 3.89$ eV) ionization potential makes it possible to obtain a high charge density $n_e$ at moderate temperatures, ensuring by the same token an appreciable value of the plasma interaction parameter $\Gamma = (8\pi)^{1/2}e^3n_e^{1/3}/(kT)^{3/2}$ [1]. The low binding energy, and hence also the relatively low (for metals) critical parameters make it possible to carry out measurements under static conditions [2-4] down to the critical point (the regions CP, 1, 2, 3, in Fig. 1). Higher temperatures and pressures are attained by pulsed isentropic compression of dense cesium vapor in the parameter region 4 on Fig. 1, where in view of the negligible ($\lesssim 0.05$) degree of ionization the decisive role is played by the interaction between the charges and the neutrals. Further increase of the degree of ionization calls for an appreciable energy input, which is effectively ensured by using dynamic methods of compression and irreversible heating of the cesium vapor in the front of a strong shock wave. [1]

We present here the results of a detailed investigation of the equation of state of a cesium plasma in the phase diagram region (6, 7 in Fig. 1) that is optimal from the point of view of displaying effects of Coulomb non-ideality. Measurements of the mechanical characteristics of shock compression, performed on heated diaphragmed shock tubes, [1,6] determine directly the caloric equation of state of the plasma. Thermodynamically self-contained information was obtained by using a two-dimensional rational-fraction approximation of the experimental data followed by integration of the differential equation of the second law of thermodynamics. [7] The caloric and thermal forms of the equation of state are compared with the theoretical models of a non-ideal plasma.

## 2. PRODUCTION AND DIAGNOSTICS OF THE PLASMA

The experimental setup is shown in Fig. 2. The apparatus comprised a shock tube thermostatically maintained at temperatures $T_0 = 450$ to $650°$C, with its low-pressure chamber filled with cesium vapor. [1,6] The propelling gas was helium, argon, or a mixture of the two, so that it was possible to vary the intensities of the shock waves in a wide range. The following parameters were registered in the experiment: the initial pressure $P_0$ and temperature $T_0$ of the cesium vapor, the shock-wave front velocity U, and the densities $\rho_1$ and $\rho_2$ ($\rho = V^{-1}$) of the plasma produced behind the incident shock wave and the reflected one. The density $\rho_1$ was measured by the pulsed x-ray diffraction method [8,6] in two sections of the shock tube, so that the stationarity of the plasma flow could be monitored on the basis of the measurements (see the characteristic oscillograms of the x-ray absorption in Fig. 3). In addition, by increasing the working voltage of the RT-2 x-ray tube to optimal value [8] 32.5 kV, we were able to increase appreciably the accuracy of the measurements of $\rho_2$ behind the reflected shock wave (Fig. 3b).

The accuracy with which the shock-compression parameters was measured was estimated by registering

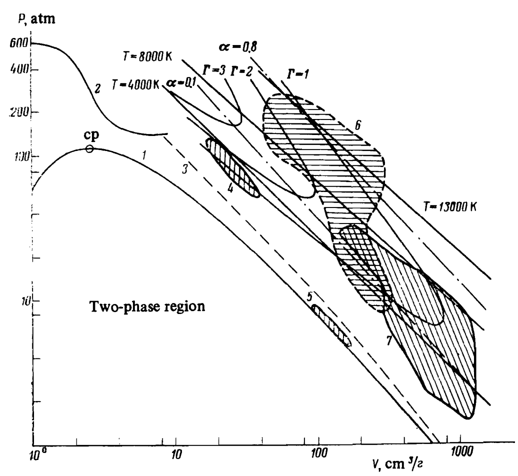


FIG. 1. Phase diagram of cesium: 1—saturation curve, static experiments, 2—[3], 3—[2,4]; 4, 5—regions of isentropic compression [4] and of the initial state, [5], 6, 7—regions of reflected and incident shock waves; Γ—non-ideality parameter, α—degree of plasma ionization.

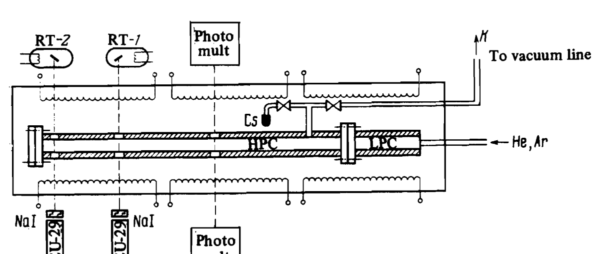


FIG. 2. Diagram of experimental setup. HPC, LPC—high- and low-pressure chambers.

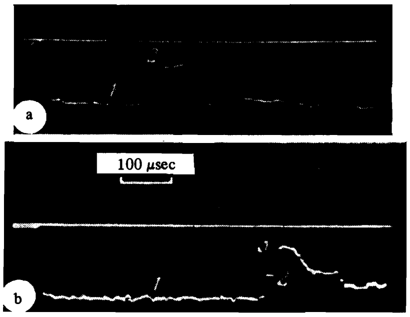


FIG. 3. Oscillograms of x-ray absorption in the first (a) and second (b) sections: 1—signal prior to arrival of shock wave, 2, 3—density discontinuity behind the incident wave and the reflected wave.

the characteristics of the reliably calculated (in view of the low degree of ionization) shock waves in xenon:

$$\Delta U/U=\pm 1\%,\quad \Delta\rho_1/\rho_1=\pm 4\%,\quad \Delta\rho_2/\rho_2=\pm 6\%.$$

The errors in the measurements of the initial parameters are $\Delta T_0/T_0 = \pm 1\%$ and $\Delta P_0/P_0 = \pm 1$ to $2\%$ (depending on $P_0$), which correspond to an accuracy $\Delta\rho_0/\rho_0 = \pm(2-3)\%$ in the density determined from these data.

## 3. CALORIC EQUATION OF STATE

The laws of mass, momentum, and energy conservation on the front of a planar stationary shock discontinuity [9]

$$P_1=P_0+\frac{U^2}{V_0}\left(1-\frac{V_1}{V_0}\right),\quad H_1=H_0+\frac{U^2}{2}\left[1-\left(\frac{V_1}{V_0}\right)^2\right],$$
$$P_2=P_1+\frac{U^2}{V_1}\left[\frac{1-(V_1/V_0)^2}{1-V_2/V_1}\right],\quad H_2=H_1+\frac{U^2}{2}\frac{(1-V_1/V_0)^2}{1-V_2/V_1}\left(1+\frac{V_2}{V_1}\right) \tag{1}$$

make it possible, given the initial conditions, to determine the pressure P and the enthalpy H from the experimentally measured $U_1$, $V_1$, and $V_2$ for each plasma state, i.e., they yield information on the caloric equation of state $H = H(P, V)$ of the shock-compressed plasma. The accuracy of the determination of the thermodynamic characteristics of the plasma from (1), in accordance with the experimental errors, is

$$\frac{\Delta P_1}{P_1}\sim\pm 3\%,\quad \frac{\Delta H_1}{H_1}\sim\pm 2\%,\quad \frac{\Delta P_2}{P_2}\sim\pm 6\%,\quad \frac{\Delta H_2}{H_2}\sim\pm 5\%.$$

The experiments were performed under initial conditions $P_0 = 0.04$ to $0.54$ bar and at shock-wave intensities $M \approx 3$ to $8$, corresponding to states in a wide region of the phase diagram of cesium (see 6 and 7 in Fig. 1). The parameters of the most typical experimental data are listed in Tables I and II, which show a comparison of the experimental data (I) with the Debye theory in a grand canonical ensemble (II) and in the ideal-gas approximation (III) with the atomic partition function $Q_{Cs} = 2$. [10] The present results, in contrast to those of [1], are typified by two circumstances: better accuracy and much wider range of measurements. It is important that in the region of the phase diagram the parameters behind the incident and reflected shock waves overlap in part. Additional proof of the reliability of the obtained data is the agreement between the specific enthalpy behind very weak shock waves with $H = (5/2)PV$, corresponding to ideal non-ionized gas. We note that despite the appreciable values of Γ, the influence of the plasma non-ideality is negligible in this range of parameters, in view of the low degree of ionization.

As seen from the table, the experimental values of the specific enthalpy H are systematically lower than those obtained from the Debye theory. At the same time, in almost all the points there is good agreement with the rather rough ideal-plasma approximation III. A similar behavior was observed in [1], but here it is more strongly pronounced in a much wider range of plasma states. To illustrate this fact, Figs. 4 and 5 show the experimental isochors $V = 200\ \mathrm{cm^3/g}$ and $V = 1000\ \mathrm{cm^3/g}$, which lie between the asymptotic curves for the ideal gas $H = (5/2)PV$ and for a fully ionized ideal plasma, $H = (5/2)PV + I/\mu$ ($\mu$ is the atomic weight of cesium). The experimental curves I in Figs. 4 and 5 were obtained from the energy surface $H = H(P, V)$ constructed as a result of a statistical reduction of the entire aggregate of the experimental data (see Sec. 4 for details). It follows from the plots in Figs. 4 and 5 that the disparity between experiment and the Debye theory first increases with increasing PV (i.e., with increasing temperature and hence with increasing degree of ionization), then decreases as complete ionization is approached, and becomes smaller than the measurement error on the upper section of the isochores. A comparison of the experimental data with other models of an ideal plasma (Figs. 4a and 5a) shows that none, with the exception of model III, agrees with experiment. From among the considered approximations, the best description of the caloric data is reached by model III of an ideal plasma with $Q_{Cs} = 2$. The small deviation from experiment observed in this case at $H \geq 4.5\times 10^{10}$ erg/g occurs in the region of measurements behind the reflected wave, where the measurement accuracy is lower, and Figs. 4 and 5 show the rms errors for the entire aggregate of the experimental data.

TABLE I. Thermodynamic parameters of cesium behind the incident shock wave.

| Experiment I | | | | | | | Theory | | | | | | |
|---|---|---|---|---|---|---|---|---|---|---|---|---|---|
| | | | | | | | III | | | | | II | |
| $P_0$, atm | $T_0$, K | $U$, km/sec | $V_1$, cm³/g | $P_1$, atm | $H_1\cdot 10^{-9}$, erg/g | $T_1$, K | $H\cdot 10^{-9}$, erg/g | $n_e\cdot 10^{-18}$, cm⁻³ | α | Γ | $T$, K | $H\cdot 10^{-9}$, erg/g | $T$, K |
| 0.130 | 780 | 0,83 | 1200 | 1,40 | 4,20 | 2600 | 4.10 | 0,006 | 0.002 | 0.20 | 2600 | 4,20 | 2600 |
| 0,147 | 780 | 0.935 | 1000 | 2,00 | 5,10 | 3100 | 5.10 | 0.03 | 0.007 | 0.34 | 3100 | 5,40 | 3100 |
| 0.107 | 760 | 1.23 | 1030 | 2.80 | 8.3 | 4100 | 8.6 | 0.250 | 0.056 | 0,62 | 4200 | 10.0 | 4200 |
| 0.160 | 780 | 1.05 | 800 | 2,90 | 6.3 | 3500 | 6.0 | 0.09 | 0.015 | 0.48 | 3500 | 6,6 | 3500 |
| 0.074 | 750 | 1,53 | 1160 | 3.10 | 12.4 | 5100 | 13.0 | 0.56 | 0.140 | 0,73 | 5000 | 15,7 | 5000 |
| 0,240 | 830 | 0.95 | 630 | 3,30 | 5,30 | 3200 | 5.20 | 0.046 | 0.006 | 0,41 | 3200 | 5,50 | 3200 |
| 0,063 | 740 | 1,87 | 1060 | 4.20 | 18,0 | 5600 | 18,0 | 1.05 | 0,250 | 0.83 | 5700 | 22.0 | 5700 |
| 0,051 | 700 | 2.23 | 1130 | 5,1 | 25,0 | 6400 | 25.6 | 1,60 | 0.41 | 0,85 | 6400 | 30,0 | 6600 |
| 0.180 | 790 | 1.33 | 580 | 5.4 | 9.6 | 4600 | 9.5 | 0.53 | 0.070 | 0,8 | 4600 | 9,5 | 4600 |
| 0,380 | 860 | 1.03 | 390 | 6,0 | 6.2 | 3600 | 6.0 | 0.13 | 0.01 | 0,59 | 3600 | 6.5 | 3600 |
| 0.078 | 750 | 2.10 | 800 | 6.5 | 22.4 | 6100 | 22.0 | 1.80 | 0.320 | 0,93 | 6200 | 26,4 | 6300 |
| 0,080 | 740 | 2,05 | 770 | 6.6 | 21.6 | 6100 | 21.0 | 1,70 | 0.290 | 0.94 | 6100 | 25,4 | 6200 |
| 0,044 | 690 | 2,77 | 1270 | 6,9 | 39.0 | 7900 | 41.0 | 2,50 | 0,70 | 0,76 | 8000 | 44.0 | 8500 |
| 0,180 | 790 | 1,49 | 530 | 7.0 | 11,8 | 5200 | 12.3 | 1.00 | 0.12 | 0.93 | 5200 | 15,6 | 5200 |
| 0,056 | 710 | 2.50 | 950 | 7.1 | 32.0 | 7000 | 31.0 | 2,40 | 0,50 | 0.89 | 7000 | 35.0 | 7300 |
| 0.044 | 690 | 2.83 | 1260 | 7.2 | 40,0 | 8100 | 43.0 | 2,60 | 0.73 | 0,75 | 8200 | 45.0 | 8700 |
| 0.240 | 820 | 1.55 | 410 | 9.4 | 12.7 | 5500 | 13.2 | 1,45 | 0,130 | 1.04 | 5400 | 17.0 | 5400 |
| 0.290 | 840 | 1.49 | 350 | 10.4 | 12.0 | 5300 | 11,7 | 1.30 | 0,10 | 1.05 | 5200 | 15.0 | 5200 |
| 0.360 | 860 | 1.92 | 240 | 22.0 | 19.0 | 6700 | 20.0 | 4.60 | 0,24 | 1.35 | 6700 | 25,0 | 6800 |
| 0.440 | 870 | 1.87 | 200 | 25.0 | 18.0 | 6700 | 18.3 | 4,80 | 0.21 | 1.40 | 6600 | 24,0 | 6600 |

TABLE II. Thermodynamic parameters of cesium behind the reflected shock wave.

| Experiment I | | | | | | | | Theory | | | | | | |
|---|---|---|---|---|---|---|---|---|---|---|---|---|---|---|
| | | | | | | | | III | | | | | II | |
| $P_0$, atm | $T_0$, K | $U$, km/sec | $V_1$, cm³/g | $V_2$, cm³/g | $P_2$, atm | $H_2\cdot 10^{-9}$, erg/g | $T_2$, K | $H\cdot 10^{-9}$, erg/g | $n_e\cdot 10^{-18}$, cm⁻³ | α | Γ | $T$, K | $H\cdot 10^{-9}$, erg/g | $T$, K |
| 0.230 | 820 | 0,90 | 680 | 250 | 12.0 | 9,0 | 4400 | 8,5 | 0.75 | 0.04 | 1.0 | 4500 | 10,4 | 4500 |
| 0.155 | 790 | 1.10 | 820 | 260 | 15.0 | 13 | 5600 | 13 | 2.1 | 0.12 | 1,2 | 5600 | 17,0 | 5600 |
| 0,094 | 760 | 1.94 | 700 | 170 | 60 | 42 | 9600 | 42 | 16 | 0.60 | 1.4 | 9900 | 45 | 10700 |
| 0,047 | 690 | 2.52 | 1150 | 300 | 64 | 73 | 15600 | 74 | 14 | 0.95 | 0,66 | 15700 | 73 | 17300 |
| 0,166 | 790 | 1.70 | 450 | 110 | 70 | 32 | 8500 | 30 | 16 | 0.38 | 1,7 | 8600 | 35.0 | 9000 |
| 0.320 | 840 | 1.58 | 280 | 75 | 95 | 27 | 8700 | 26 | 19 | 0.32 | 1.9 | 8500 | 33.0 | 8800 |
| 0.180 | 800 | 1.96 | 420 | 100 | 100 | 42 | 10000 | 41 | 25 | 0.56 | 1.6 | 10300 | 44 | 11000 |
| 0,064 | 710 | 2.75 | 860 | 240 | 104 | 90 | 19700 | 90 | 19 | 0,97 | 0.54 | 19500 | 85 | 21400 |
| 0.130 | 790 | 2.30 | 490 | 144 | 130 | 64 | 15200 | 71 | 28 | 0.90 | 0,95 | 15500 | 70 | 17400 |
| 0.440 | 870 | 1.87 | 190 | 50 | 200 | 38 | 11000 | 37 | 43 | 0.45 | 2.1 | 10500 | 41 | 11200 |

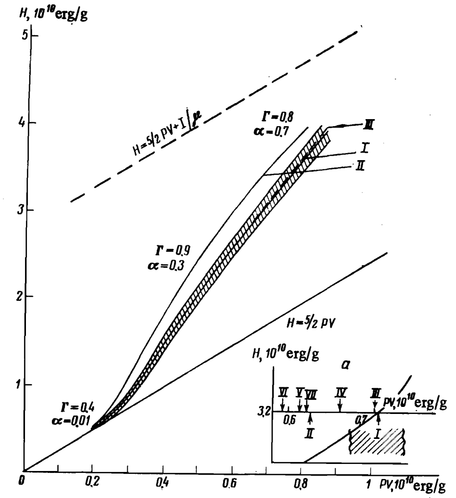

FIG. 4. Isochore of cesium plasma $V = 10^3$ cm$^3$/g. The error corridor is shaded.

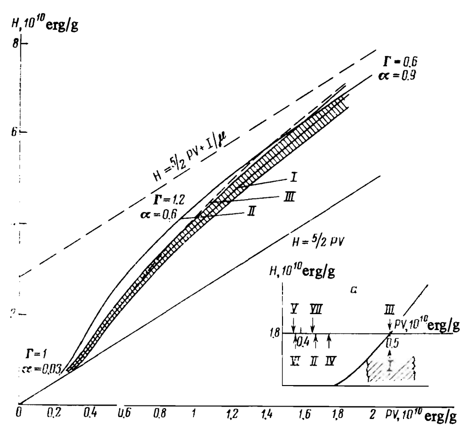

FIG. 5. Cesium plasma isochore $V = 200$ cm$^3$/g. The error corridor is shaded.

## 4. THERMODYNAMICALLY COMPLETE EQUATION OF STATE

Since the enthalpy H is not a thermodynamic potential with respect to the PV variables, to obtain thermodynamically complete information from the dynamic experiments it is necessary to have additionally [7], besides $H + H(P, V)$, the expression for the temperature of this shock-compressed medium $T = T(P, V)$. The optical opacity of the saturated vapors in a dense cesium plasma does not make it possible [1] to register T directly at the same time that the mechanical parameters of the shock compression are measured. To construct a thermodynamically closed equation of state, we used a semi-empirical method [7,9] that employs of caloric shock-wave information and isentrope relations that follow from the second law of thermodynamics (it is more convenient to introduce in lieu of H the internal energy $E = H - PV$):

$$E=E_0\exp\left\{-\int_{V_0}^{V}\gamma(V,E)\,d\ln V\right\}; \qquad (2)$$

$$T=T_0\frac{PV}{P_0V_0}\exp\left\{-\int_{V_0}^{V}\left(\frac{\partial\ln\gamma(V,E)}{\partial\ln V}\right)_E d\ln V\right\}, \qquad (3)$$

where

$$\gamma(V,E)=PV/E \qquad (4)$$

is an analog of the Grüneisen coefficient.

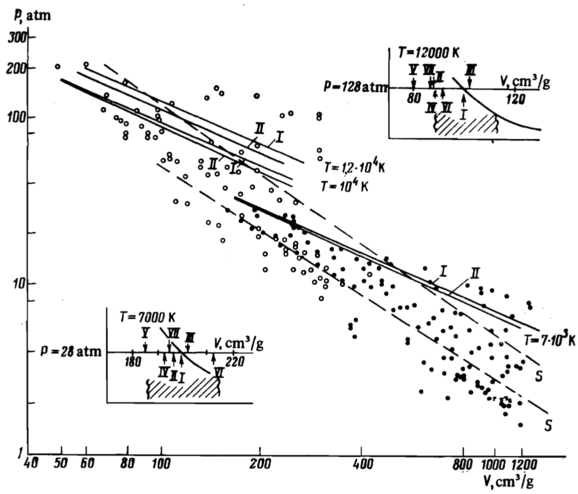

FIG. 6. Isotherms of cesium plasma T; S—isentropes, •—incident shock wave, ○—reflected shock wave.

The system (2) and (3) was supplemented by the following initial conditions: the temperature $T_0$ and energy $E_0$ were specified on the $V_0 = 1600$ cm$^3$/g isochore. The lower isentropes (Fig. 6) emerge in this case to the region of the non-ionized gas, where $PV = RT$, while the temperature on the ends of the upper isentropes was determined in accord with model III, chosen because its caloric equation $H(P, V)$ agrees well with experiment in the neighboring measured region $V \sim 1300$ cm$^3$/g.

To calculate the temperature in the entire investigated range of parameters it is necessary that the corresponding isentropes (2) and (3) pass through those parts of the phase diagram where the experimental results have been obtained. The derivative $(\partial \ln \gamma/\partial \ln V)_E$ which enters in (3) can be reliably calculated in the case when the aggregate of the experimental points is large enough in terms of the variables E and V. At the same time, a decisive role is played by the tendency to obtain information at the highest possible non-ideality parameters.

The aggregate of the experimental data obtained in accordance with these considerations is represented in the PV plane in Figs. 1 and 6. It is seen that the experiments cover the phase-diagram region that is optimal for the separation of the Coulomb-interaction effects.

In order to describe jointly the experimental data on the direct and reflected shock waves in a wide range of the phase diagram it is necessary to have mathematical expressions having stable approximation properties. The representation of the energy surface in the form (4) leads to a slight change of $\gamma(E, V)$ with an appreciable variation of E and V, and is therefore convenient for interpolation, the plasma interaction changes $\gamma(E, V)$ from 2/3 to ~1/5. The initial experimental information $\{\gamma_k \pm \sigma_k;\ V_k,\ E_k\}_{k=1}^{N}$ is approximated by the Padé representation

$$\gamma(V,E)=R(V,E)/Q(V,E), \qquad (5)$$

where $R(V, E)$ and $Q(V, E)$ are polynomials of the type

$$\sum_{i+j\le m,n} a_{ij}(\ln V)^i(\ln E)^j.$$

The coefficients $a_{ij}$ minimize the nonlinear functional

$$S=\sum_{N} g_k^2[\gamma_k-\gamma(V_k,E_k)]^2 \qquad (6)$$

with weights $g_k \sim \sigma_k^{-1}$. The powers m and n in (5) are chosen by analyzing the experimental data on the basis of the Fisher's statistical significance criterion.[7] We assumed m = n = 2, which corresponds to 12 coefficients $a_{ij}$ in (5).

An estimate of the temperature-calculation accuracy $\Delta T/T$ as a function of the expected experimental errors and the inaccuracies with which the initial data are specified was obtained by varying the corresponding data and by stimulating statistically, with a computer, the probability structure of the measurement process.[7] For the isotherms $T = 7 \times 10^3$, $10^4$, and $1.2 \times 10^{4}$°K, the errors $\Delta T/T$ were estimated at 5, 7, and 8%, respectively. The increase in the error is due to the smaller number of data at the edges of the aggregate of the experimental data (Fig. 6) and to the large uncertainty in the specification of the initial conditions for the upper isotherms.

The isotherms of a non-ideal partially-ionized plasma, obtained from (2)–(6), are shown in Fig. 6. We note that the experimental points demonstrate here the uniformity with which the investigated region is filled, and not the scatter of the points relative to the isotherms, inasmuch as the temperatures are different at different points. Figure 6 shows also a comparison with the extrapolation into the strongly-non-ideal region of the parameters, of a number of most typical theoretical models.[1)] Besides the traditional approximations[10] (model of an ideal plasma with a kT bound on $Q_{Cs}$ (IV), the Debye theory in small (V) and grand (II) ensembles of statistical mechanics), we used also some of the recent data on model analysis and of calculations by the Monte Carlo method. The use of the Monte Carlo method to calculate a partly-ionized plasma entails difficulties in the description of quantum effects of the electron-ion interaction.[11] Concrete results can therefore be obtained[12] only for the pseudopotential model of a plasma (index IV), based on a special choice of the effective interaction of the electron-ion pair interaction. In our calculations of the equation of state we used polynomial approximations of the numerical data.[12] Allowance for the normalization condition[13] that reflects the screening of an arbitrary charge in a plasma[14,15] leads to a noticeable improvement of the extrapolation properties of the Debye approximation (VII) and can serve as a basis for the development of model equations of state.

The presented interpretation of the experimental data shows that most employed theoretical models do not contradict, within the limits of the estimated accuracy, the experimental isotherms of the cesium plasma. However, only in the ideal-plasma model (III) with $C_{Cs} = 2$ are the descriptions of the caloric and thermal equations of state H(P, V) and T(P, V) in agreement. Thus, in an experimental verification of the various theoretical approximations it is necessary, above all, to compare H = H(P, V) with the obtained experimental data, and ensure at the same time that the description of the thermal plasma characteristics T = T(P, V) are not contradictory. Calculations carried out within the framework of the indicated approximations show that agreement with experiment can be reached only by imposing a very strong limitation on the contribution of the bound states ($Q_{Cs} = 2$). At the same time, the correction to the equation of state for the interaction of the free charges should be much lower than the Debye correction. It is possible that an appreciable decrease of the energy contribution of the bound states to the enthalpy, together with the decrease of the correction for the interaction of the free charges in the equation of state, is due to the deformation and to the distortion of the energy levels at high densities. A quantitative description of this phenomenon calls for complicated self-consistent quantum-mechanical calculations[16] with introduction of special assumptions concerning the character of the interparticle interaction in the system.

We note in conclusion that the character of the obtained experimental curves, and also the absence of various types of hydrodynamic anomalies,[17] offer evidence of a uniform phase composition of the plasma[18] in the investigated wide range of parameters.

We are deeply grateful to L. V. Al'tshuler for interest and support, and to I. L. Iosilevskiĭ and V. K. Gryaznov for theoretical calculations and discussions.

[1)]The calculations were performed by I. L. Isilevskiĭ and V. K. Gryaznov.


[1] V. N. Lomakin and V. E. Fortrov, Zh. Eksp. Teor. Fiz. **63**, 92 (1972) [Sov. Phys.-JETP **36**, 48 (1973)]; Dokl. Akad. Nauk SSSR **206**, 576 (1972) [Sov. Phys. Dokl. **17**, 889 (1973)].

[2] R. G. Gross and D. A. Greenwood, Prog. Mater. Sci. **14**, 173 (1971).

[3] V. A. Alekseev, V. G. Ocharenko, Yu. F. Ryzhkov, and A. P. Senchenkov, Pis'ma Zh. Eksp. Teor. Fiz. **12**, 306 (1970) [JETP Lett. **12**, 207 (1970)].

[4] Yu. S. Korshukov, A. P. Senchenkov, E. I. Asinovskii, and A. T. Kunavin, Teplofiz. Vys. Temp. **6**, 1288 (1970).

[5] A. G. Kunavin, A. V. Kirillin, and Yu. S. Korshunov, Teplofiz. Vys. Temp. **13**, 1304 (1974).

[6] V. A. Sechenov and O. E. Shchekotov, Teplofiz. Vys. Temp. **12**, 652 (1974).

[7] V. E. Fortov and Yu. G. Krasnikov, Zh. Eksp. Teor. Fiz. **59**, 1645 (1970) [Sov. Phys.-JETP **32**, 897 (1971)]; I. I. Sharipdzhakov, A. V. Bushman, L. V. Al'tshuler, and V. E. Fortov, Doklad na V Vsesoyuzoĭ konferentsii po teplofizicheskim svoĭstvam veshchestv (Paper at 5th All-Union Conf. on Thermophys. Prop. of Materials), Kiev, 1974.

[8] B. N. Lomakin and V. E. Fortov, Teplofiz. Vys. Temp. **9**, 66 (1971).

[9] Ya. B. Zel'dovich and Yu. P. Raĭzer, Fizika udarnykh voln i vysokotemperaturnykh gidrodinamicheskikh yavleniĭ (Physics of Shock Waves and High Temp. Hydrodynamic Phenomena), Nauka, 1966.

[10] V. E. Fortov, B. H. Lomakin, and Yu. G. Krasnikov, Teplofiz. Vys. Temp. **9**, 869 (1971).

[11] G. É. Norman, in: Ocherki fiziki i khimii nizkotemperaturnoĭ plazmy (Outlines of Physics and Chemistry of Low Temp. Plasma), ed. L. S. Polak, Nauka, 1971, p. 260.

[12] B. V. Zelener, G. É. Norman, and V. S. Filinov, Teplofiz. Vys. Temp. **10**, 1160 (1972).

[13] V. K. Gryaznov and I. L. Iosilevskiĭ, Chislennye metody mekhaniki sploshnoĭ sredy (Numerical Methods of Mech. of Solid Media) **4**, 166 (1973).

[14] F. H. Stillinger and R. Lowett, J. Chem. Phys. **49**, 1991 (1968).

[15] G. A. Martynov, Zh. Eksp. Teor. Fiz. **54**, 159 (1968) [Sov. Phys.-JETP **27**, 87 (1968)].

[16] V. K. Gryasnov, A. N. Ivanova, and V. E. Fortov, 12th Conf. on Phenomena in Ionized Gases, Eindhoven, 1975.

[17] V. E. Fortov, Teplofiz. Vys. Temp. **10**, 168 (1972).

[18] G. E. Hofman and A. N. Starostin, Teplofiz. Vys. Temp. **8**, 413 (1970).


Translated by J. G. Adashko
175